Meshless local collocation method for natural frequencies and mode shapes of laminated composite shells

Song Xiang[*1] and Ying-tao Chen[2]

[1]*Liaoning Key Laboratory of General Aviation, Shenyang Aerospace University, No. 37 Daoyi South Avenue, Shenyang, Liaoning, 110136, People's Republic of China*
[2]*Faculty of Aerospace engineering, Shenyang Aerospace University, No. 37 Daoyi South Avenue, Shenyang, Liaoning, 110136, People's Republic of China*

Abstract.   Meshless local collocation method produces much better conditioned matrices than meshless global collocation methods. In this paper, the meshless local collocation method based on thin plate spline radial basis function and first-order shear deformation theory are used to calculate the natural frequencies and mode shapes of laminated composite shells. Through numerical experiments, the accuracy and efficiency of present method are demonstrated.

Keywords: meshless local collocation; thin plate spline; radial basis function; natural frequencies; mode shapes; laminated composite shell

1. Introduction

The increased usage of laminated composite shells in the aerospace, pressure vessels, ship, building, and many other structures has generated much interest in free vibration behavior of composite shell.

Reddy and Liu (1985) developed a higher-order shear deformation theory for bending and natural vibration of laminated shells under simply supported boundary conditions. Their theory was a modification of the Sanders' theory and accounted for parabolic distribution of the transverse shear strains through thickness of the shell and tangential stress-free boundary conditions on the boundary surfaces of the shell. Toorani and Lakis (2006) studied the free vibrations of non-uniform composite cylindrical shells. Korhevskaya and Mikhasev (2006) studied the free vibrations of a laminated cylindrical shell subjected to nonuniformly distributed axial forces. Hu and Ou (2001) maximized the fundamental frequencies of laminated truncated conical shells with respect to fiber orientation by using a sequential linear programming method with a simple move-limit strategy. Timarchi and Soldatos (2000) studied the free vibrations of finite, closed, circular cylindrical shells, made of one or more monoclinic layers. Their study was based on the Love-type version of a unified shear-deformable shell theory. Ferreira *et al*. (2007) evaluated the natural frequencies of doubly curved cross-ply composite shells by the first-order

---

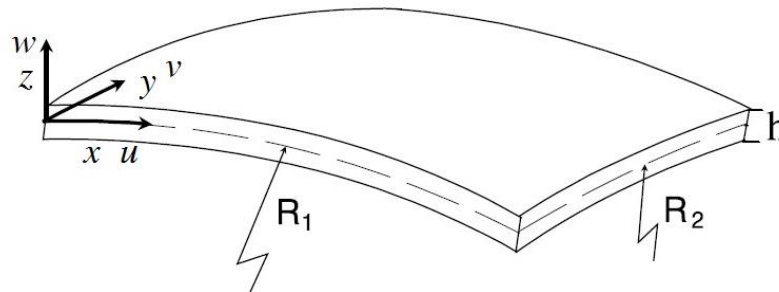*Corresponding author, Professor, E-mail: xs74342@sina.com

Fig. 1 Schematic of a shell

theory of Donnell and a meshless method based on multiquadric radial basis functions. Ferreira *et al*. (2011a) performed the static and free vibration analysis of laminated shells by radial basis functions collocation and a sinusoidal shear deformation theory. Mantari *et al*. (2012) presented the bending and free vibration analysis of multilayered plates and shells by using a new accurate higher order shear deformation theory (HSDT). Ferreira *et al*. (2011b) computed the static deformations and the natural frequencies of doubly-curved composite shells by the first-order theory of Donnell and a meshless method based on wavelet collocation. Topal (2013) studied the Pareto optimum design of laminated composite truncated circular conical shells.

Meshless methods based on collocation techniques include meshless global collocation method and meshless local collocation method. The meshless global collocation method approximates the solution of partial differential equations using all nodes in the problem domain. But global collocation method can result in fully populated coefficient matrices and only deal with the problem with regular geometry. Local collocation method constructs the approximation function using the nodes in the support domain of any data center and requires only inversion of matrices of small size which is equal to the number of nodes in the support domain. Lee *et al*. (2003) presented a truly meshless approximation strategy for solving partial differential equations based on the local multiquadric and the local inverse multiquadric approximations. Roque *et al*. (2012) used a higher-order shear deformation plate theory and a radial basis function-finite difference technique for predicting the transient behavior of thin and thick composite plates. Roque *et al*. (2011) used a higher-order shear deformation plate theory and a radial basis function-finite difference technique for predicting the static behavior of thin and thick composite plates. Xiang *et al*. (2011a) proposed a meshless local radial point collocation method based on multiquadric radial basis function to analyze the free vibration behavior of laminated composite plates. They studied the choice of shape parameter, effect of dimensionless sizes of the support domain on accuracy and convergence characteristics. Xiang and Kang (2012) focused for the first time on free vibration analysis of laminated composite plates by a meshless local collocation method based on thin plate spline radial basis function.

According to the results of literature survey, the meshless local collocation method has not yet been utilized to predict the free vibration behavior of laminated composite shells. In the present paper, meshless local collocation method based on the thin plate spline radial basis function is used to discretize the governing equations and boundary conditions based on the first-order shear deformation shell theory. The singularity of thin plate spline radial basis function is eliminated by adding infinitesimal to the zero distance. The present results are compared with the available published results to demonstrate the numerical accuracy of present method. The aim of this paper

is to explore the potential of meshless local collocation method in the vibration analysis of laminated composite shells.

2. Governing equations based on the first-order shear deformation theory

The coordinate system and geometry of a shell are shown in Fig. 1. For the spherical shell, $R_1 = R_2 = R$. For the cylindrical shell, $R_1 = R$, $R_2 = \infty$.

The governing equations of laminated composite shells based on the first-order shear deformation theory are as follows

$$A_{11}\left(\frac{\partial^2 u}{\partial x^2} + \frac{1}{R_1}\frac{\partial w}{\partial x}\right) + A_{12}\left(\frac{\partial^2 v}{\partial x \partial y} + \frac{1}{R_2}\frac{\partial w}{\partial x}\right) + B_{11}\frac{\partial^2 \phi_x}{\partial x^2} + B_{12}\frac{\partial^2 \phi_y}{\partial x \partial y} + A_{66}\left(\frac{\partial^2 v}{\partial x \partial y} + \frac{\partial^2 u}{\partial y^2}\right)$$
$$+ B_{66}\left(\frac{\partial^2 \phi_y}{\partial x \partial y} + \frac{\partial^2 \phi_x}{\partial y^2}\right) = -I_0\omega^2 u - I_1\omega^2 \phi_x \tag{1}$$

$$A_{22}\left(\frac{\partial^2 v}{\partial y^2} + \frac{1}{R_2}\frac{\partial w}{\partial y}\right) + A_{12}\left(\frac{\partial^2 u}{\partial x \partial y} + \frac{1}{R_1}\frac{\partial w}{\partial y}\right) + B_{12}\frac{\partial^2 \phi_x}{\partial x \partial y} + B_{22}\frac{\partial^2 \phi_y}{\partial y^2} + A_{66}\left(\frac{\partial^2 v}{\partial x^2} + \frac{\partial^2 u}{\partial x \partial y}\right)$$
$$+ B_{66}\left(\frac{\partial^2 \phi_y}{\partial x^2} + \frac{\partial^2 \phi_x}{\partial x \partial y}\right) = -I_0\omega^2 v - I_1\omega^2 \phi_y \tag{2}$$

$$A_{55}\left(\frac{\partial \phi_x}{\partial x} + \frac{\partial^2 w}{\partial x^2}\right) + A_{44}\left(\frac{\partial \phi_y}{\partial y} + \frac{\partial^2 w}{\partial y^2}\right) + A_{12}\left(-\frac{2}{R_1 R_2}w - \frac{1}{R_1}\frac{\partial v}{\partial y} - \frac{1}{R_2}\frac{\partial u}{\partial x}\right)$$
$$+ \frac{A_{22}}{R_2}\left(-\frac{\partial v}{\partial y} - \frac{1}{R_2}w\right) + \frac{A_{11}}{R_1}\left(-\frac{\partial u}{\partial x} - \frac{1}{R_1}w\right) = -I_0\omega^2 w \tag{3}$$

$$A_{55}\left(-\frac{\partial w}{\partial x} - \phi_x\right) + D_{66}\left(\frac{\partial^2 \phi_x}{\partial y^2} + \frac{\partial^2 \phi_y}{\partial x \partial y}\right) + D_{12}\frac{\partial^2 \phi_y}{\partial x \partial y} + D_{11}\frac{\partial^2 \phi_x}{\partial x^2} + B_{11}\left(\frac{\partial^2 u}{\partial x^2} + \frac{1}{R_1}\frac{\partial w}{\partial x}\right) +$$
$$B_{12}\left(\frac{\partial^2 v}{\partial x \partial y} + \frac{1}{R_2}\frac{\partial w}{\partial x}\right) + B_{66}\left(\frac{\partial^2 u}{\partial y^2} + \frac{\partial^2 v}{\partial x \partial y}\right) = -I_1\omega^2 u - I_2\omega^2 \phi_x \tag{4}$$

$$A_{44}\left(-\frac{\partial w}{\partial y} - \phi_y\right) + D_{66}\left(\frac{\partial^2 \phi_y}{\partial x^2} + \frac{\partial^2 \phi_x}{\partial x \partial y}\right) + D_{12}\frac{\partial^2 \phi_x}{\partial x \partial y} + D_{22}\frac{\partial^2 \phi_y}{\partial y^2} + B_{12}\left(\frac{\partial^2 u}{\partial x \partial y} + \frac{1}{R_1}\frac{\partial w}{\partial y}\right) +$$
$$B_{22}\left(\frac{\partial^2 v}{\partial y^2} + \frac{1}{R_2}\frac{\partial w}{\partial y}\right) + B_{66}\left(\frac{\partial^2 u}{\partial x \partial y} + \frac{\partial^2 v}{\partial x^2}\right) = -I_1\omega^2 v - I_2\omega^2 \phi_y \tag{5}$$

where u, v, w, ϕ_x and ϕ_y are the unknown displacement components of middle surface of the shell. A_{ij}, B_{ij}, and D_{ij} are the stiffness components, I_i are the mass inertias.

$$A_{ij} = \sum_{k=1}^{N_L} \int_{z_k}^{z_{k+1}} \overline{Q}_{ij}^{(k)} dz \tag{6}$$

$$B_{ij} = \sum_{k=1}^{N_L} \overline{Q}_{ij}^{(k)} \int_{z_k}^{z_{k+1}} z dz \tag{7}$$

$$D_{ij} = \sum_{k=1}^{N_L} \overline{Q}_{ij}^{(k)} \int_{z_k}^{z_{k+1}} z^2 dz \tag{8}$$

$$I_0 = \int_{-\frac{h}{2}}^{\frac{h}{2}} \rho dz, I_1 = \int_{-\frac{h}{2}}^{\frac{h}{2}} \rho z dz, I_2 = \int_{-\frac{h}{2}}^{\frac{h}{2}} \rho z^2 dz \tag{9}$$

where ρ denotes the material density, N_L is total number of layer, z_k and z_{k+1} are the lower and upper z coordinates of the kth layer, $\overline{Q}_{ij}^{(k)}$ are the transformed elastic coefficients.

$$\overline{Q}_{11} = Q_{11} \cos^4 \theta + 2(Q_{12} + 2Q_{66}) \sin^2 \theta \cos^2 \theta + Q_{22} \sin^4 \theta$$

$$\overline{Q}_{12} = (Q_{11} + Q_{22} - 4Q_{66}) \sin^2 \theta \cos^2 \theta + Q_{12} (\sin^4 \theta + \cos^4 \theta)$$

$$\overline{Q}_{22} = Q_{11} \sin^4 \theta + 2(Q_{12} + 2Q_{66}) \sin^2 \theta \cos^2 \theta + Q_{22} \cos^4 \theta$$

$$\overline{Q}_{66} = (Q_{11} + Q_{22} - 2Q_{12} - 2Q_{66}) \sin^2 \theta \cos^2 \theta + Q_{66} (\sin^4 \theta + \cos^4 \theta)$$

$$\overline{Q}_{44} = Q_{44} \cos^2 \theta + Q_{55} \sin^2 \theta$$

$$\overline{Q}_{55} = Q_{55} \cos^2 \theta + Q_{44} \sin^2 \theta \tag{10}$$

where θ is the angle between 1-axis and x-axis, 1-axis being the first principal material axis, and the reduced stiffness components are given as

$$Q_{11} = \frac{E_1}{1 - v_{12}v_{21}}, Q_{22} = \frac{E_2}{1 - v_{12}v_{21}}, Q_{12} = v_{21}Q_{11}$$

$$Q_{66} = G_{12}, Q_{44} = G_{23}, Q_{55} = G_{13}, v_{21}E_1 = v_{12}E_2 \tag{11}$$

The boundary conditions for an arbitrary edge with clamped supported and simply supported are as follows

Clamped

$$u = v = w = \phi_x = \phi_y = 0 \tag{12}$$

Simply supported

$$x = 0, a : v = w = \phi_y = 0, N_x = 0, M_x = 0$$
$$y = 0, b : u = w = \phi_x = 0, N_y = 0, M_y = 0 \tag{13}$$

$$N_x = A_{11}\left(\frac{\partial u}{\partial x} + \frac{w}{R_1}\right) + A_{12}\left(\frac{\partial v}{\partial y} + \frac{w}{R_2}\right) + B_{11}\frac{\partial \phi_x}{\partial x} + B_{12}\frac{\partial \phi_y}{\partial y} \tag{14}$$

$$N_y = A_{12}\left(\frac{\partial u}{\partial x} + \frac{w}{R_1}\right) + A_{22}\left(\frac{\partial v}{\partial y} + \frac{w}{R_2}\right) + B_{12}\frac{\partial \phi_x}{\partial x} + B_{22}\frac{\partial \phi_y}{\partial y} \tag{15}$$

$$M_x = B_{11}\left(\frac{\partial u}{\partial x} + \frac{w}{R_1}\right) + B_{12}\left(\frac{\partial v}{\partial y} + \frac{w}{R_2}\right) + D_{11}\frac{\partial \phi_x}{\partial x} + D_{12}\frac{\partial \phi_y}{\partial y} \tag{16}$$

$$M_y = B_{12}\left(\frac{\partial u}{\partial x} + \frac{w}{R_1}\right) + B_{22}\left(\frac{\partial v}{\partial y} + \frac{w}{R_2}\right) + D_{12}\frac{\partial \phi_x}{\partial x} + D_{22}\frac{\partial \phi_y}{\partial y} \tag{17}$$

3. Local collocation method

The solution of Eqs. (1)-(5) and corresponding boundary conditions can be approximated with a function $U^h(X)$ using the meshless local collocation method

$$U^h(X) \approx \sum_{i=1}^{n} \alpha_i R_i + \sum_{j=1}^{m} \beta_j P_j \tag{18}$$
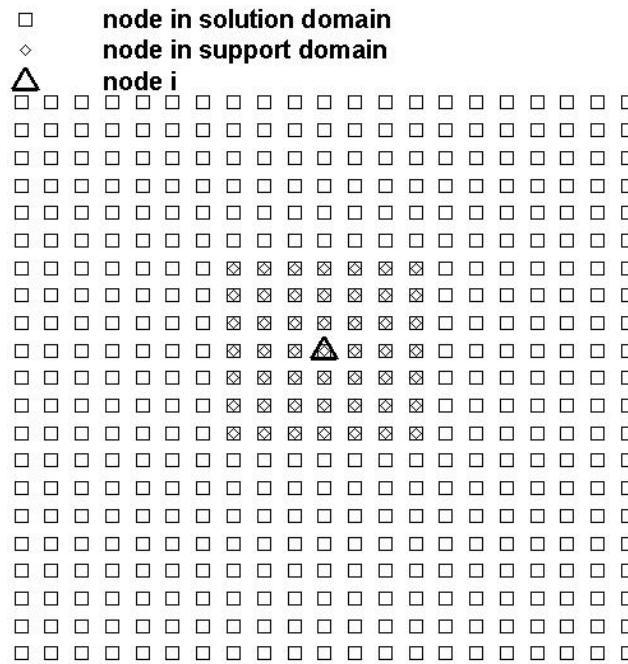

Fig. 2 The solution domain and support domain of node *i* (α_s=3)

where n is the number of nodes in the support domain, m is the number of terms of monomial, α_i and β_j are unknown coefficients, R_i is radial basis function, P_j is polynomial basis function. The size of support domain for node i is defined as

$$d_s = \alpha_s d_c \tag{19}$$

where α_s is the dimensionless sizes of the support domain, d_c is the nodal spacing. Fig. 2 shows the solution domain and support domain of node i.

In the present paper, the thin plate spline radial basis function is utilized to approximate the solution of partial differential equations. The thin plate spline is defined as follows

$$R_i = [(x-x_i)^2 + (y-y_i)^2]^k \log_{10}^{(\sqrt{(x-x_i)^2+(y-y_i)^2})} \tag{20}$$

where x_i and y_i are coordinate of node i, k is shape parameter.

The thin plate spline has the disadvantage of singularity when the distance between node i and node j is zero. when the distance between two nodes is zero, $r_{ij}^2 = r_{ji}^2 + \varsigma$. r_{ij} is the distance between node i and node j, $\varsigma = 1 \times 10^{-60}$. The infinitesimal value is obtained by numerical experiments. When the infinitesimal value ς is less than 1×10^{-60}, the eigenvalue can't be obtained.

Polynomial basis function used in this paper is as follows

$$P^T = [1, x, y] \tag{21}$$

The constraint condition is

$$P\alpha = 0 \tag{22}$$

Eq. (18) and Eq. (22) can be rewritten in matrix form by enforcing the interpolation passing through the value at all nodes in the supporting domain.

$$\begin{bmatrix} R & P^T \\ P & 0 \end{bmatrix} \begin{bmatrix} \alpha \\ \beta \end{bmatrix} = \mathbf{G}\eta = \begin{bmatrix} U_s \\ 0 \end{bmatrix} \tag{23}$$

where

$$\begin{bmatrix} R & P^T \end{bmatrix} = \begin{bmatrix} R_1(r_1) & R_1(r_2) & ... & R_1(r_n) & 1 & x_1 & y_1 \\ R_2(r_1) & R_2(r_2) & ... & R_2(r_n) & 1 & x_2 & y_2 \\ ... & ... & ... & ... & ... & ... & ... \\ R_n(r_1) & R_n(r_2) & ... & R_n(r_n) & 1 & x_n & y_n \end{bmatrix} \tag{24}$$

$$\begin{bmatrix} P & 0 \end{bmatrix} = \begin{bmatrix} 1 & 1 & ... & 1 & 0 & 0 & 0 \\ x_1 & x_2 & ... & x_n & 0 & 0 & 0 \\ y_1 & y_2 & ... & y_n & 0 & 0 & 0 \end{bmatrix} \tag{25}$$

$$\eta^T = [\alpha_1, \alpha_2, ..., \alpha_n, \beta_1, \beta_2, \beta_3] \tag{26}$$

According to the Eq. (23), the following formulation can be obtained as

$$\eta = G^{-1} \begin{bmatrix} U_s \\ 0 \end{bmatrix}$$
(27)

Substituting Eq. (27) into Eq. (18), we can obtain the following equation

$$U(X) = \Phi_s U_e$$
(28)

where Φ_s is the shape function, U_e is the nodal displacement.

$$\Phi_s = [R(r_1), R(r_2), ..., R(r_n), 1, x, y]G^{-1}$$
(29)

$$U_e^T = [U_1, U_2, ..., U_n, 0, 0, 0]$$
(30)

The shape function Φ_s obtained through the local collocation method possesses delta function properties.

4. Discretization of governing equations and boundary conditions

The displacement function at a point X can be approximated as

$$\begin{bmatrix} u \\ v \\ w \\ \phi_x \\ \phi_y \end{bmatrix} = \begin{bmatrix} \Phi_1 & 0 & 0 & 0 & 0 & ... & \Phi_N & 0 & 0 & 0 & 0 \\ 0 & \Phi_1 & 0 & 0 & 0 & ... & 0 & \Phi_N & 0 & 0 & 0 \\ 0 & 0 & \Phi_1 & 0 & 0 & ... & 0 & 0 & \Phi_N & 0 & 0 \\ 0 & 0 & 0 & \Phi_1 & 0 & ... & 0 & 0 & 0 & \Phi_N & 0 \\ 0 & 0 & 0 & 0 & \Phi_1 & ... & 0 & 0 & 0 & 0 & \Phi_N \end{bmatrix} \begin{bmatrix} u_1 \\ v_1 \\ w_1 \\ \phi_{x1} \\ \phi_{y1} \\ ... \\ u_N \\ v_N \\ w_N \\ \phi_{xN} \\ \phi_{yN} \end{bmatrix} = \begin{bmatrix} \Phi_u \\ \Phi_v \\ \Phi_w \\ \Phi_{\phi_x} \\ \Phi_{\phi_y} \end{bmatrix} U_n$$
(31)

where N is the total number of nodes in the entire problem domain.

The discretized governing equations can be obtained by substituting Eq. (31) and their derivatives into Eqs. (1)-(5). Corresponding boundary conditions can be discretized in a similar way.

The discretized governing equations and boundary conditions can be expressed as:

$$\begin{bmatrix} L\Phi \\ B\Phi \end{bmatrix} U_n = \omega^2 \begin{bmatrix} \Phi \\ 0 \end{bmatrix} U_n$$
(32)

Then

$$\begin{bmatrix} L\Phi \\ B\Phi \end{bmatrix}^{-1} \begin{bmatrix} \Phi \\ 0 \end{bmatrix} U_n = \frac{1}{\omega^2} U_n \tag{33}$$

where L and B are the differential operator, $1/\omega^2$ is eigenvalue, U_n is eigenvector. Eigenvalue $1/\omega^2$ in Eq. (33) can be solved by a standard eigenvalue solver.

5. Numerical examples

The dimensionless sizes α_s and shape parameter k have the important effect on the accuracy of local collocation method based on thin plate spline radial basis function. Xiang and Kang (2012) performed the free vibration analysis of laminated composite plates by a meshless local collocation method based on thin plate spline radial basis function. In their study, $\alpha_s=5$ and $k=3$ produced the better results. Therefore, α_s and k of the present paper are the same as Xiang and Kang (2012).

The relative material properties of a layer are as follows

$$E_1 = 25E_2, G_{12} = G_{13} = 0.5E_2, G_{23} = 0.2E_2, v_{12} = 0.25, \rho = 1$$

The frequency is non-dimensionalized by Eq. (34)

$$\bar{\omega} = \omega(a^2/h)\sqrt{\rho/E_2} \tag{34}$$

5.1 Convergence study

Figs. 3-4 show the non-dimensional fundamental frequency of the laminated composite shells $(0°/90°/90°/0°)$ as the grid distribution is increased from 13×13 to 21×21. Figs. 5-6 show the non-
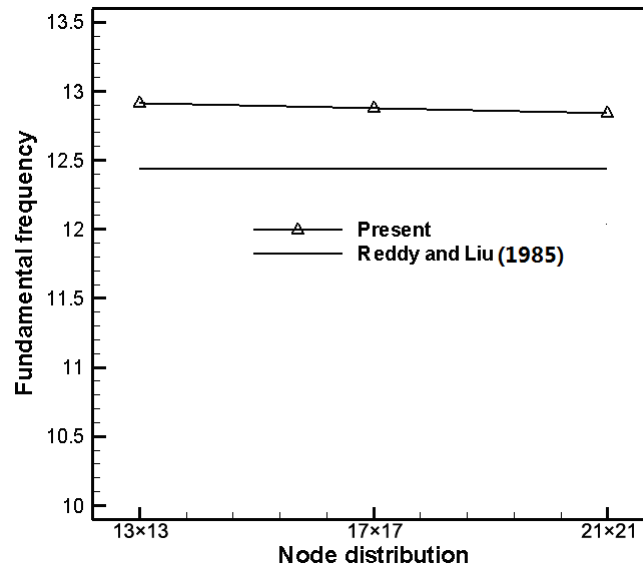

Fig. 3 Convergence study of non-dimensionalized fundamental frequency of simply supported laminated composite spherical shells $(0°/90°/90°/0°)$ ($a/h=10$, $R/a=5$)
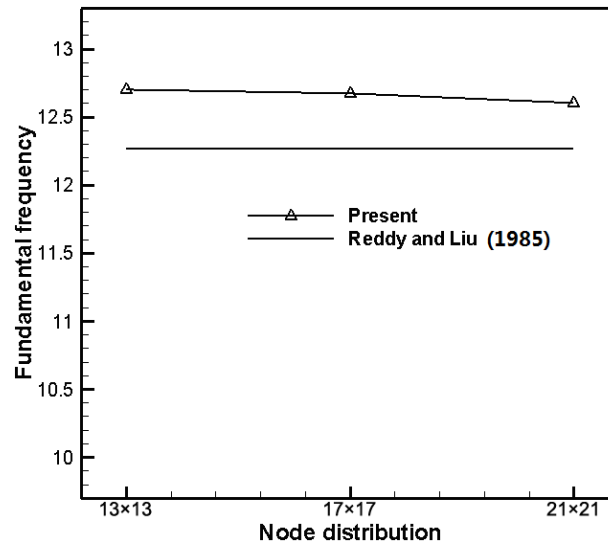
Fig. 4 Convergence study of non-dimensionalized fundamental frequency of simply supported laminated composite cylindrical shells (0°/90°/90°/0°) (*a/h*=10, *R/a*=5)
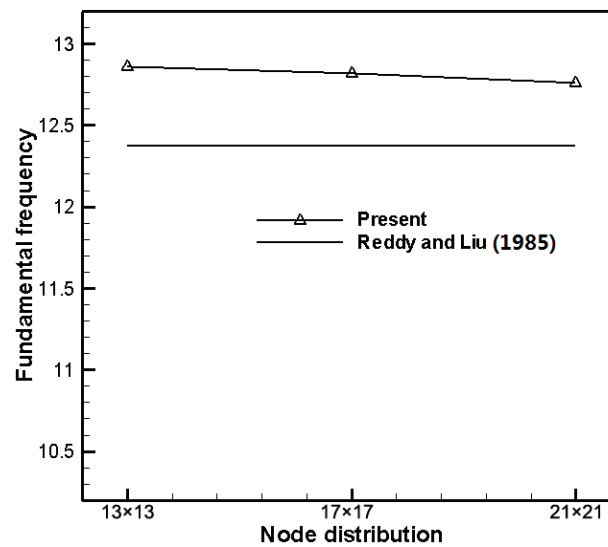

Fig. 5 Convergence study of non-dimensionalized fundamental frequency of simply supported laminated composite spherical shells (0°/90°/0°) (*a/h*=10, *R/a*=5)

dimensional fundamental frequency of the laminated composite shells (0°/90°/0°) as the grid distribution is increased from 13×13 to 21×21. Good convergence characteristics are observed for all considered problems.

5.2 Comparison study

According to the results of convergence study, the 21×21 regular grid pattern is adopted. The

non-dimensionalized fundamental frequencies of laminated composite spherical shells are listed in Tables 1-2 and compared with the results of Reddy and Liu (1985), Ferreira *et al.* (2007), Xiang *et al.* (2011b).

The non-dimensionalized fundamental frequencies of laminated composite cylindrical shells are listed in Tables 3-4 and compared with the results of Reddy and Liu (1985), Ferreira *et al.* (2007), Xiang *et al.* (2011b).

It is found from Tables 1-4 that present results are in good agreement with those of available published results.

Fig. 7 shows the variation of non-dimensionalized fundamental frequency of simply supported laminated composite spherical shells under *R/a* (0°/90°/90°/0°, *a/h*=10). Fig. 8 shows the variation
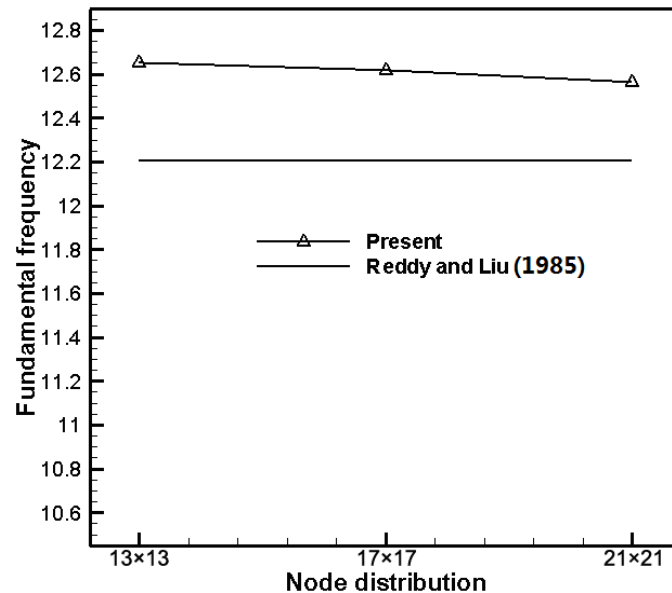

Fig. 6 Convergence study of non-dimensionalized fundamental frequency of simply supported laminated composite cylindrical shells (0°/90°/0°) (*a/h*=10, *R/a*=5)

Table 1 Non-dimensionalized fundamental frequency of simply supported laminated composite spherical shells (0°/90°/90°/0°)

a/h	Method	*R/a*				
		5	10	20	50	100
10	Reddy and Liu (1985)	12.437	12.280	12.240	12.229	12.228
	Ferreira *et al.* (2007)	12.493	12.299	12.250	12.236	12.234
	Xiang *et al.* (2011b)	12.845	12.656	12.608	12.594	12.592
	Present	12.836	12.644	12.595	12.582	12.580
100	Reddy and Liu (1985)	31.079	20.380	16.638	15.426	15.245
	Ferreira *et al.* (2007)	31.296	20.422	16.601	15.363	15.173
	Xiang *et al.* (2011b)	31.645	20.714	16.993	15.704	15.522
	Present	31.647	20.893	17.150	15.943	15.763

Table 2 Non-dimensional fundamental frequency of simply supported laminated composite spherical shells (0°/90°/0°)

a/h	Method	R/a				
		5	10	20	50	100
10	Reddy and Liu (1985)	12.372	12.215	12.176	12.165	12.163
	Ferreira *et al*. (2007)	12.428	12.234	12.185	12.171	12.169
	Xiang *et al*. (2011b)	12.791	12.602	12.553	12.540	12.538
	Present	12.758	12.587	12.543	12.531	12.529
100	Reddy and Liu (1985)	30.993	20.347	16.627	15.424	15.244
	Ferreira *et al*. (2007)	31.214	20.393	16.594	15.362	15.177
	Xiang *et al*. (2011b)	31.595	20.723	16.871	15.644	15.493
	Present	30.850	20.605	17.055	15.916	15.746

Table 3 Non-dimensional fundamental frequency of simply supported laminated composite cylindrical shells (0°/90°/90°/0°)

a/h	Method	R/a				
		5	10	20	50	100
10	Reddy and Liu (1985)	12.267	12.236	12.230	12.228	12.227
	Ferreira *et al*. (2007)	12.2943	12.2515	11.7827	12.2377	12.2373
	Xiang *et al*. (2011b)	12.646	12.605	12.595	12.592	12.592
	Present	12.605	12.585	12.581	12.579	12.579
100	Reddy and Liu (1985)	20.361	16.634	15.559	15.245	15.199
	Ferreira *et al*. (2007)	20.5928	16.6203	15.5093	15.1249	15.0754
	Xiang *et al*. (2011b)	20.881	17.108	15.820	15.526	15.474
	Present	19.525	16.646	15.938	15.741	15.712

Table 4 Non-dimensionalized fundamental frequency of simply supported laminated composite cylindrical shells (0°/90°/0°)

a/h	Method	R/a				
		5	10	20	50	100
10	Reddy and Liu (1985)	12.207	12.173	12.166	12.163	12.163
	Ferreira *et al*. (2007)	12.2309	12.1871	12.1720	12.1730	12.1726
	Xiang *et al*. (2011b)	12.594	12.552	12.541	12.538	12.537
	Present	12.564	12.538	12.531	12.529	12.529
100	Reddy and Liu (1985)	20.332	16.625	15.556	15.224	15.198
	Ferreira *et al*. (2007)	20.6684	16.6494	15.5113	15.1331	15.0836
	Xiang *et al*. (2011b)	21.076	17.075	15.786	15.575	15.603
	Present	20.339	16.998	16.028	15.744	15.703

of non-dimensionalized fundamental frequency of simply supported laminated composite cylindrical shells under R/a (0°/90°/90°/0°, a/h=10). According to the Figs 7-8, the non-dimensionalized fundamental frequencies decrease with the increase of R/a.

The present method produces very stable and well defined mode shapes, as shown in Figs. 9-10.

6. Conclusions

Meshless local collocation method based on the thin plate spline radial basis function is used to discretize the governing equations and boundary conditions based on the first-order shear
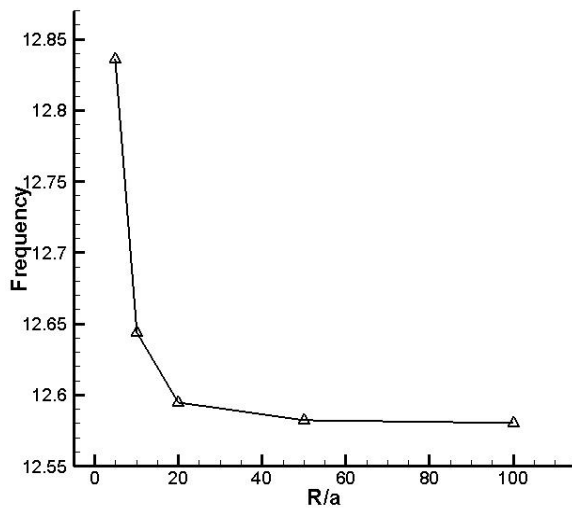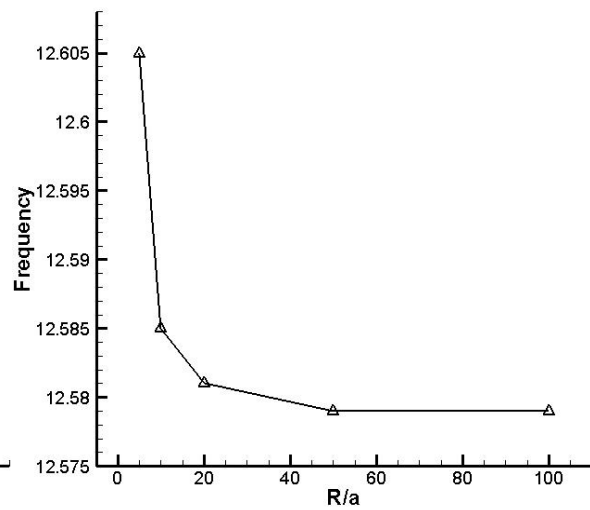

Fig. 7 Variation of non-dimensionalized fundamental frequency of simply supported laminated composite spherical shells under *R/a* (0°/90°/90°/0°, *a/h*=10)

Fig. 8 Variation of non-dimensionalized fundamental frequency of simply supported laminated composite cylindrical shells under *R/a* (0°/90°/90°/0°, *a/h*=10)
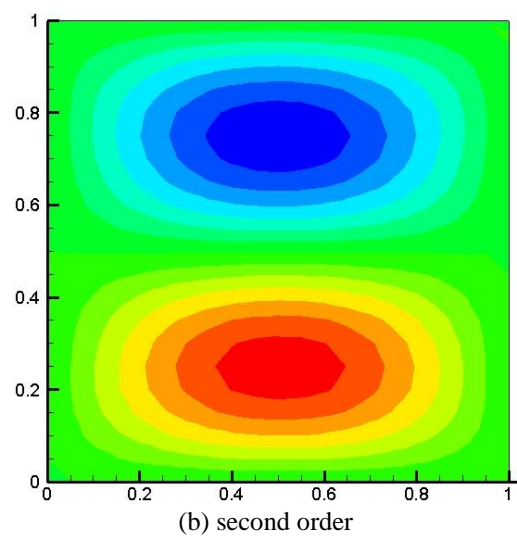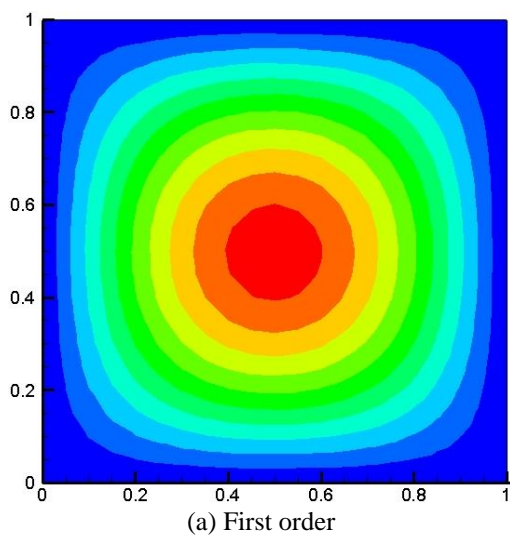

(a) First order

(b) second order

Fig. 9 First 4 mode shapes for spherical shell with a/h=100, R/a=10 (0°/90°/90°/0°)

(c) Third order

(d) Fourth order

Fig. 9 Continued

(a) First order

(b) second order

(c) Third order

(d) Fourth order
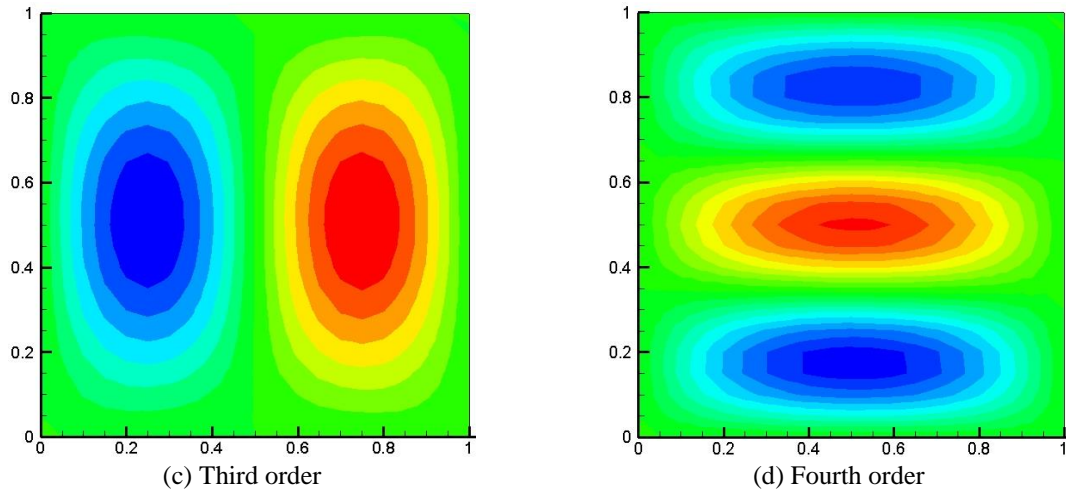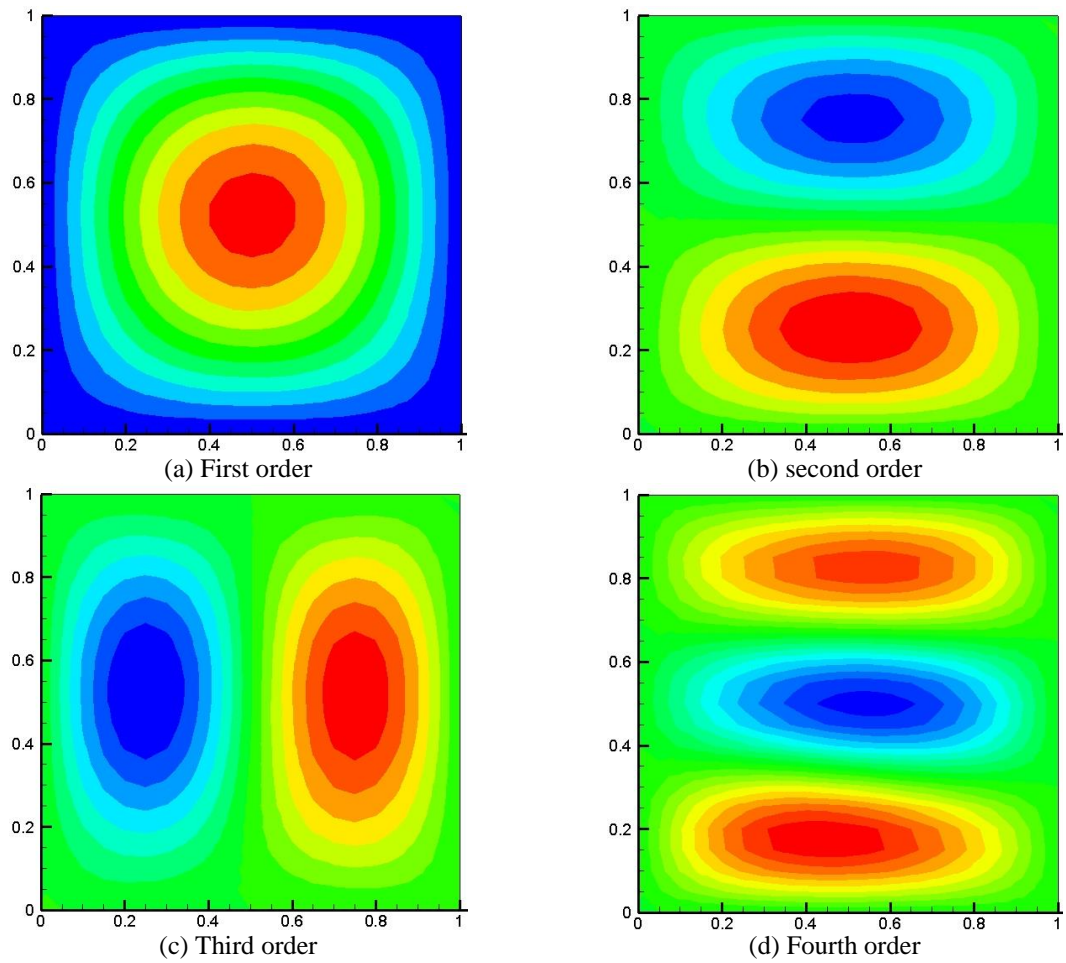
Fig. 10 First 4 mode shapes for cylindrical shell with a/h=100, R/a=10 (0°/90°/90°/0°)

eformation shell theory. The singularity of thin plate spline radial basis function is eliminated by adding infinitesimal to the zero distance. The present results are compared with the available published result which demonstrates the potential of meshless local collocation method in the vibration analysis of laminated composite shells.

Acknowledgments

References

Ferreira, A.J.M., Roque, C.M.C. and Jorge, R.M.N. (2007), "Natural frequencies of FSDT cross-ply composite shell by multiquadrics", *Compos. Struct.*, **77**, 296-305.

Ferreira, A.J.M., Carrera, E., Cinefra, M., Roque, C.M.C. and Polit, O. (2011a), "Analysis of laminated shells by a sinusoidal shear deformation theory and radial basis functions collocation, accounting for through-the-thickness deformations", *Compos. Part B*, **42**, 1276-1284.

Ferreira, A.J.M., Castro, L.M. and Bertoluzza, S. (2011b), "A wavelet collocation approach for the analysis of laminated shells", *Compos. Part B*, **42**(1), 99-104.

Hu, H.T. and Ou, S.C. (2001), "Maximizations of fundamental frequency of laminated truncated conical shells with respect to fiber orientation", *Compos. Struct.*, **52**, 265-275.

Korhevskaya, E.A. and Mikhasev, G.I. (2006), "Free vibrations of a laminated cylindrical shell subjected to nonuniformly distributed axial forces", *Mech. Solid.*, **41**, 130-138.

Lee, C.K., Liu, X. and Fan, S.C. (2003), "Local multiquadric approximation for solving boundary value problems", *Comput. Mech.*, **30**, 396-409.

Mantari, J.L., Oktem, A.S. and Soares, C.G. (2012), "Bending and free vibration analysis of isotropic and multilayered plates and shells by using a new accurate higher-order shear deformation theory", *Compos. Part B*, **43**(8), 3348-3360.

Reddy, J.N. and Liu, C.F. (1985), "A higher-order shear deformation theory of laminated elastic shells", *Int. J. Eng. Sci.*, **23**, 319-330.

Roque, C.M.C., Cunha, D., Shu, C. and Ferreira, A.J.M. (2011), "A local radial basis functions-finite differences technique for the analysis of composite plates", *Eng. Anal. Bound. Elem.*, **35**, 363-374.

Roque, C.M.C., Cunha, D. and Ferreira, A.J.M. (2012), "Transient analysis of composite plates by a local radial basis functions-finite difference technique", *Acta Mechanica Solida Sinica*, **25**(1), 22-36.

Timarchi, T. and Soldatos, K.P. (2000), "Vibrations of angle-ply laminated circular cylindrical shells subjected to different sets of edge boundary conditions", *J. Eng. Math.*, **37**, 211-230.

Toorani, M.H. and Lakis, A.A. (2006), "Free vibrations of non-uniform composite cylindrical shells", *Nucl. Eng. Des.*, **236**, 1748-1758.

Topal, U. (2013), "Pareto optimum design of laminated composite truncated circular conical shells", *Steel Compos. Struct.*, **14**(4), 397-408.

Xiang, S., Li, G.C., Zhang, W. and Yang, M.S. (2011a), "A meshless local radial point collocation method for free vibration analysis of laminated composite plates", *Compos. Struct.*, **93**, 280-286.

Xiang, S., Bi, Z.Y., Jiang, S.X., Jin, Y.X. and Yang, M.S. (2011b), "Thin plate spline radial basis function for the free vibration analysis of laminated composite shells", *Compos. Struct.*, **93**, 611-615.

Xiang, S. and Kang, G.W. (2012), "Local thin plate spline collocation for free vibration analysis of laminated composite plates", *Eur. J. Mech. A/Solid.*, **33**, 24-30.

Notations

u	displacement in x direction
v	displacement in y direction
w	displacement in z direction
ϕ_x	rotations
A_{ij}, B_{ij}, D_{ij}	stiffness components
I_i	mass inertias
ρ	material density
N_L	total number of layer
$\overline{Q}_{ij}^{(k)}$	transformed elastic coefficients
θ	the angle between 1-axis and x-axis
n	the number of nodes in the support domain
R_i	radial basis function
P_j	polynomial basis function
α_s	dimensionless sizes of the support domain
d_c	nodal spacing
x_i and y_i	coordinate of node i
r_{ij}	distance between node i and node j
Φ_s	shape function
U_e	nodal displacement
ω	natural circular frequency